CrossMark

ORIGINAL ARTICLE

Estimation of metabolic rate from activity measured by recorders deployed on Japanese sea bass *Lateolabrax japonicus*

Tomohiko Mori[1] · **Naoyuki Miyata**[1] · **Jun Aoyama**[1] · **Yasuaki Niizuma**[2] ·
Katsufumi Sato[1]

Abstract Understanding the energy expenditure of top predators is important because a collapse in them could trigger trophic cascades through ecosystems. One such top predator, Japanese sea bass *Lateolabrax japonicus*, helps to balance the structure of the coastal marine ecosystem through predation. In this study, accelerometry was applied to the Japanese sea bass to estimate its energy expenditure under natural conditions. We attached accelerometers to five wild fish and measured metabolic rates such as the oxygen consumption rate ($\dot{V}O_2$, mg O_2 kg^{-1} min^{-1}) using a swim tunnel. Body beat frequency (BBF) was measured using the accelerometer. The BBF was correlated with the tail beat frequency (TBF) by analyzing video recordings. $\dot{V}O_2$ was related to swimming speed (U), TBF, and BBF. We estimated the standard (45.9 kJ kg^{-1} day^{-1}) and active (124.0 kJ kg^{-1} day^{-1}) metabolic rates when fish were not swimming and when they were swimming at the optimum swimming speed, respectively. The energy required to compensate for the above metabolic rates are between 83.3 and 275.6 kJ kg^{-1} day^{-1} using an assimilation efficiency of 0.7 and assuming that the growth rate is zero. These costs were comparable to consuming one or two prey fish per day (e.g., Japanese sardine: mean total length $155 \pm$ SD 6 mm).

Introduction

Top-level predators play a significant role in balancing the whole structure of the aquatic ecosystem by foraging on lower-level organisms [1]. For example, Frank et al. [2] reported the collapse of Atlantic cod *Gadus morhua* and several other species that are top predators of fish and microinvertebrates in the continental-shelf ecosystem. The associated trophic cascade, which was caused by overexploitation of the benthic fish community, coincided with increased abundances of small pelagic fishes and benthic macroinvertebrates (crabs and shrimps) and also with a decline in the zooplankton in the Eastern Scotian Shelf ecosystem, Canada. On the other hand, increased predation by killer whales probably caused a decline in sea otter numbers which led to an increase in sea urchin abundance (sea otter prey) and thus the disappearance of kelp forests (sea urchin food) [3]. A collapse in top predators can cause a trophic cascade that affects the ecosystem at all levels. Such predator–prey interactions can be described as energy flows. These fluctuations in the abundance and changes in the amount of energy consumed by top predators were very important influence through the coastal and offshore ecosystems [1–3]. Therefore, evaluating the energy requirements of top predators represents the first step towards understanding the energy flow in an ecosystem. The amount of energy required by a predatory fish is described by the following equation [4]:

$$C = R + E + P,$$

✉ Tomohiko Mori
isana-137@aori.u-tokyo.ac.jp

1 Atmosphere and Ocean Research Institute, The University of Tokyo, 5-1-5 Kashiwanoha, Kashiwa, Chiba 277-8564, Japan

2 Laboratory of Environmental Zoology, Faculty of Agriculture, Meijo University, 1-501 Shiogamakuchi, Tenpaku-ku, Nagoya, Aichi 468-8502, Japan

where *C* is the total quantity of prey energy consumed by a predator, *R* is the energy consumed by a predator that is used by it for respiration (total metabolism), *E* is the energy content of products excreted by the predator (i.e., feces and urine), and *P* is the metabolic production costs for the predator (i.e., for growth and reproduction) [4]. Note that *R* includes both physiological and kinematic costs. In ectotherms, the physiological cost is affected by the temperature. The resting metabolic rate and swimming ability of fish have been found to increase as the water temperature increases, up to an optimum temperature [5]. The kinematic locomotion cost, which depends on the activity of the animal, is more variable than the physiological cost. Energetic studies on fishes have traditionally been conducted using respirometry in a swim tunnel to measure the dissolved oxygen concentration in the water [5–9]. It has been found that swimming speed is strongly positively correlated to oxygen consumption rate [4]. In addition, tail beat frequency, heart rate, and dynamic body acceleration (DBA) are strong predictors of the oxygen consumption rate [4, 10–12]. There have recently been many studies that have used DBA parameters, especially overall dynamic body acceleration (ODBA) and the vector of the DBA (VeDBA), as proxies for activity and to estimate energy expenditure [13–16].

Activity-related parameters such as the swimming speed, tail beat frequency, and DBA of free-ranging fish have been recorded using animal-borne devices, which can also simultaneously record environmental variables [17, 18]. Therefore, it is possible to estimate the energy expenditure of free-ranging fish from time-series information on activity and environmental variables (especially temperature) by instrumenting the animals with appropriate data loggers or acoustic transmitters [11, 16, 19, 20].

Japanese sea bass *Lateolabrax japonicus* is an abundant top-level predator in estuarine and coastal ecosystems in Japan [21]. It lives in fresh water, brackish water, and seawater (it is amphidromous). It is commercially fished using trawl, round haul, and gill nets, especially in Tokyo Bay, Japan [22]. It can grow to >1 m in total length and is a popular catch in sports fishing. It feeds on fish, crustaceans, and polychaeta. As it matures it becames more piscivorous [23]. Some previous studies have investigated the feeding habits [24, 25], distribution [26, 27], and migration [24, 28] of larval and juvenile Japanese sea bass. Nevertheless, only a few studies have considered the energetics of adult Japanese sea bass [29, 30].

In the study reported in the present paper, accelerometry was applied to estimate the oxygen consumption rate of Japanese sea bass using relationships between activity parameters (swimming speed, tail beat frequency, body beat frequency, and DBA), and the feasibility of using these activity parameters to estimate the energy expenditure of Japanese sea bass in subsequent field studies was evaluated. In addition, we attempted to quantify the energetic requirements of sea bass (assuming no growth) and to estimate the number of prey species that a sea bass consumes per day.

Materials and methods

Respirometry experiments

Respirometry experiments were conducted in August–November 2012 and November–December 2014. We captured Japanese sea bass (*n* = 5, total length 344–461 mm, body mass 0.35–0.83 kg) using fishing gear around Banzu tidal flats (35°26′N, 139°53′E) at Kisarazu City, Chiba, and the estuaries of the Arakawa and Kyu-Edogawa rivers (35°38′N, 139°52′E), Edogawa-ku, Tokyo, Japan. Fish were transported in a 500-l seawater tank to the Atmosphere and Ocean Research Institute, University of Tokyo, at Kashiwa City, Chiba, Japan. There, fish were acclimated in a circular 1000-l seawater tank for several weeks. The circular tank was maintained at 20 °C using a temperature control system in an air-conditioned room. Fish were fed on Japanese anchovy *Engraulis japonicus* 4–5 times per week. Japanese sea bass were fasted for a total of two days before respirometry trials.

Before transferring them into the swim tunnel, each fish was anesthetized with 0.1–0.5 ‰ 2-phenoxyethanol, and then its total length and body mass were measured to the nearest 1 mm and 10 g, respectively. Two small holes (ca. 2 mm in diameter) were then drilled into the body near the base of the first dorsal fin, and an accelerometer (ORI400-D3GT: 45 mm length, 12 mm diameter, 10 g in air, Little Leonardo Ltd., Tokyo, Japan) was attached in front of the first dorsal fin using two plastic cables that were passed through the holes. After it had recovered from the anesthesia, each fish was placed in a 127-l Blazka-type swim tunnel, as described by Van den Thillart et al. [9]. This swim tunnel has one propeller at the end of the tunnel that controls the flow speed of the water (Fig. 1). The dissolved oxygen level in each swim tunnel was continuously measured using an oxygen sensor (InPro6050 series, Mettler Toledo Inc., Greifensee, Switzerland) in a 1-l cylinder tube (Fig. 1) and then recorded on a computer using Labview software (National Instruments Co., Tokyo, Japan). The oxygen level varied between 100 and 60 % oxygen saturation during respirometry trials. The water in the flush tank was saturated with oxygen and circulated between the swim tunnel and the tank. In each respirometry trial, water in the swim tunnel was circulated in closed condition by closing the valves on the tubes connected to the flush tank (Fig. 1). Dissolved oxygen gradually decreased due to the
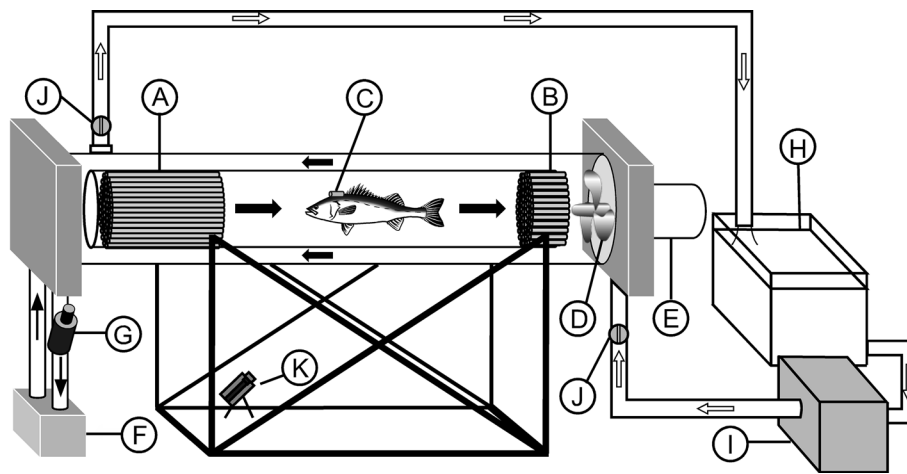
Fig. 1 Schematic diagram of a Blazka-type swim tunnel *A* and *B* PVC stream tube, *C* accelerometer, *D* propeller, *E* electromotor, *F* pump, *G* dissolved oxygen sensor, *H* 240-l flush tank, *I* temperature control system with pump, *J* valve, *K* digital high-vision video camera with infrared light. *Closed* and *open arrows* show the direc-tions of water flow during measurements of the oxygen consumption rate and during flushing, respectively. At the end of the swim tunnel, water flows down through the dissolved oxygen sensor and is returned to the swim tunnel via a pump

respiration of the fish, so the oxygen consumption rate ($\dot{V}O_2$, mg O_2 kg^{-1} min^{-1}) was calculated via

$$\dot{V}O_2 = 127\Delta O_2 \Delta t^{-1} BM^{-1}, \tag{1}$$

where $\Delta O_2 \Delta t^{-1}$ is the average decrease in dissolved oxygen (mg O_2 l^{-1}) within the respirometry system over time (min) and BM is the body mass of the fish (kg).

Before $\dot{V}O_2$ measurements were performed, each fish instrumented with an accelerometer was placed in the swim tunnel with water flowing at a speed of 0.2 m s^{-1} for an acclimation period of at least 24 h. During this acclimation period, the fish hovered and swam intermittently, so we defined this behavior as corresponding to static conditions. After the acclimation period, $\dot{V}O_2$ measurements were initiated at a flow speed of 0.1 m s^{-1}. Each run proceeded for 30–60 min in darkness (to exclude any observer effects). The flow speed was increased stepwise by 0.1 or 0.2 m s^{-1} in subsequent runs. After each $\dot{V}O_2$ measurement, the valves on the tubes were opened and the water was recirculated between the swim tunnel and the flush tank to reoxygenate the water. The fish were then rested for 30–60 min at 0.2 m s^{-1}. All $\dot{V}O_2$ measurements were conducted until a flow speed of 0.9 m s^{-1} was attained or the fish was fatigued (i.e., the fish was pressed against the PVC stream tube at the end of the swim tunnel). During all $\dot{V}O_2$ measurements, the behavior of the fish was recorded by a digital HD video camera (HDR-CX700, Sony Co., Tokyo, Japan) in night mode with an infrared light. In addition, the tail beat frequency (TBF) was measured for the first 5 min of each HD video recording of fish behavior. When the fish was fatigued and could not swim continuously in the swim tunnel, the measurements taken during that period were

excluded from the analysis. The water temperature was kept constant at 20.7 ± 0.1 °C by the temperature control system in the pump and an air conditioner in the experiment room. In the present study we used the relative swimming speed (*U*: body length per second, BL s^{-1}) instead of the swimming speed (m s^{-1}) to account for variations in fish body size.

Swimming ability of Japanese sea bass

$\dot{V}O_2$ was fitted to *U*, TBF, and body beat frequency (BBF), calculated as described below, by exponential regression [16]:

$$\dot{V}O_2 = \exp(a + bX), \tag{2}$$

where *a* and *b* are constants and *X* is the variable (i.e., *U*, TBF, or BBF). We used generalized linear mixed models (GLMM) to estimate these parameters. We used the function glmer, in the lme4 package of the R (version 3.0.2) statistical software environment, using fish ID as a random effect. We also calculated dynamic body acceleration parameters (ODBA and VeDBA) using methods employed in previous studies [13, 15, 16], and then fitted them to $\dot{V}O_2$ with

$$\dot{V}O_2 = c + dZ, \tag{3}$$

where *c* and *d* are constants and *Z* is the variable (ODBA or VeDBA). Finally, we compared models using Akaike's information criterion (AIC).

Resting metabolic rate (RMR), which is the metabolic rate of the stationary fish (i.e., when it was not swimming), was difficult to measure accurately using our respirometry

system. Thus, the oxygen consumption rate at a swimming speed of zero was considered to be the standard metabolic rate (SMR) [4].

To evaluate the swimming efficiency of Japanese sea bass, $\dot{V}O_2$ was converted into the cost of transport (COT, J kg^{-1} km^{-1}) using an oxycalorific value of 14.1 J mg O$_2^{-1}$ [4]. Furthermore, the optimum swimming speed (U_{opt}) was estimated as the swimming speed at which the COT was minimized (COT$_{min}$). COT was calculated with the same parameters (a and b) included in Eq. 2 using the following equation [4]:

$$COT = \frac{\exp(a + bU)}{U}. \tag{4}$$

The metabolic rate when the fish swim at U_{opt} was defined as the active metabolic rate (AMR$_{opt}$). SMR and AMR$_{opt}$ were also converted into daily metabolic rates (kJ kg^{-1} day^{-1}) using the oxycalorific value.

Data logger and analysis

We used a triaxial accelerometer in the $\dot{V}O_2$ measurements. This accelerometer recorded depth, temperature, and triaxial (lateral, longitudinal, and dorsoventral) accelerations. Depth and temperature data were recorded at a frequency of 1 Hz and acceleration data were recorded at a frequency of 20 Hz. The measurement ranges were from 0 to 400 m for depth, from −20 to 50 °C for temperature, and ±4 g (ca. 39.2 m s^{-2}) for acceleration.

To analyze the swimming data for the fish, we used the Ethographer [31] for IGOR Pro software, version 6.2.2 (WaveMetrics, Lake Oswego, OR, USA). Ethographer can generate spectrograms of lateral acceleration for frequency spectrum analysis with wavelet transformation. We generated a spectrogram from the raw lateral acceleration (ranging from 0.3 to 10 Hz) based on continuous wavelet transformation, and then grouped the data into 1-s intervals. Next, the dominant frequency of lateral acceleration was calculated using the peak tracer function in Ethographer. Peak tracer can extract the peak of the dominant cycle of acceleration every 1 s. Then we set the threshold entropy of peak tracer for each individual at 0.90–0.96 to remove noise and weak lateral acceleration signals. We assumed that the reciprocal of the dominant cycle was the dominant frequency (Hz) of lateral movement for the fish (BBF). BBF corresponds to movement recorded by the attached point accelerometer, and is not the same as TBF. It is impossible to measure TBF directly using an accelerometer. Therefore, we calculated a regression line between BBF and TBF to estimate the TBF of fish under natural conditions.

ODBA and VeDBA were calculated using methods utilized in previous studies [15, 16]. In order to estimate the static acceleration component of the raw acceleration along each axis, a running mean of 2 s was used. Dynamic acceleration was calculated by subtracting the static acceleration from the raw acceleration along each axis. Indices of dynamic body acceleration were calculated using the following equations:

$$ODBA = |Ax| + |Ay| + |Az|, \tag{5}$$

$$VeDBA = \sqrt{Ax^2 + Ay^2 + Az^2}, \tag{6}$$

where Ax, Ay, and Az are the dynamic accelerations along the lateral, longitudinal, and dorsoventral axes, respectively. The mean ODBA and VeDBA were calculated every 2 s. The time taken to measure each $\dot{V}O_2$ value was used to extract the mean ODBA and VeDBA values over the corresponding time period.

Measuring the calorific value each prey item

Various prey items of Japanese sea bass were reported by Miyahara et al. [23], and other prey species were collected around estuarine and coastal areas in Oita prefecture, Japan, using fishing gear and by fishermen using purse seining. Prey items were frozen and sent to our laboratory. After thawing out the prey samples, body length and wet mass were measured to the nearest 1 mm and 0.1 g, respectively. They were then dried for 24–48 h using an automatic oven (DX302, Yamato Scientific Co., Ltd., Tokyo, Japan), and dry mass was measured to the nearest 0.01 g. Finally, the calorific value of each was measured (in J per 1 g dry mass) using a bomb calorimeter (C2000 basic, IKA-Werke, Offenburg, Germany).

Results

Swimming ability

A total of 26 measurements from five fish were used for analysis (Table 1). All fish were alive after the respirometry experiments. Three of the fish were fatigued when the swimming speed was 2.0 BL s^{-1} (TBF: 2.7–3.0 Hz). The fish displayed unsteady swimming (alternating swimming and coasting), with their pectoral fins fluttering, when the swimming speed was less than 0.5 BL s^{-1} (TBF <1.2 Hz, Table 2). The fish adopted steady swimming by undulating their caudal fin continuously when the swimming speed was between 0.7 and 1.5 BL s^{-1} (1.5–2.4 Hz), except for the biggest individual, no. 5 (Tables 1, 2). When the fish swam at speeds >1.5 BL s^{-1} (2.4–2.7 Hz), they adopted burst-and-glide swimming, except in the case of no. 5 (Table 2).

The relationship between swimming speed (U) and oxygen consumption rate $\dot{V}O_2$ was fitted using Eq. 2 [$\dot{V}O_2 = \exp(0.815 + 0.686\ U)$, $n = 26$, Fig. 2a]. Furthermore,

Table 1 Details of the Japanese sea bass used in the respirometry measurements

ID no.	Total length (mm)	Body mass (kg)	SMR (mg O_2 kg^{-1} min^{-1})	U_{opt} (BL s^{-1})	COT$_{min}$ (J kg^{-1} km^{-1})	Acclimated temperature (°C)	Number of measurements
1	344	0.35	2.26	1.7	2514	20.8	3 (1)
2	454	0.65	1.54	0.9	2538	20.7	4 (1)
3	428	0.53	1.96	1.1	2158	20.7	4 (1)
4	382	0.49	2.46	1.8	2722	20.6	9
5	461	0.83	1.86	1.3	2374	20.9	6
Mean	414	0.57	2.26	1.5	2390	20.7	

Number in parentheses indicates the number of measurements excluded from the analysis due to fish fatigue

Table 2 Swimming patterns of Japanese sea bass used in respirometry measurements at each swimming speed

ID no.	<0.5 BL s^{-1} (<1.2 Hz)	0.7–1.0 BL s^{-1} (1.5–1.9 Hz)	1.1–1.5 BL s^{-1} (2.0–2.4 Hz)	1.5–2.0 BL s^{-1} (2.4–2.7 Hz)	2.1–2.3 BL^{-1} (2.7–3.0 Hz)
1	NA	S	S	B	B
2	U	S	S	B	B
3	U	S	S	B	B
4	U	S	S	B	B
5	S	NA	S	S	B

Ranges in parentheses indicate the mean tail beat frequencies observed in video recording at each swimming speed

U unsteady swimming with pectoral fin, *S* steady swimming with caudal fin, *B* burst-and-glide swimming, *NA* not available

the mean TBF determined from the video recordings and the BBF calculated from lateral acceleration were also fitted to $\dot{V}O_2$ using Eq. 2 [$\dot{V}O_2 = \exp(0.292 + 0.632\,\text{TBF})$, $n = 26$, Fig. 2b] and [$\dot{V}O_2 = \exp(0.497 + 0.518\,\text{BBF})$, $n = 26$, Fig. 2c]. The mean VeDBA and ODBA calculated via Eqs. 4 and 5, respectively, were also fitted to $\dot{V}O_2$ using Eq. 3 ($\dot{V}O_2 = 1.794 + 115.30\,\text{ODBA}$, $n = 26$, Fig. 3a; and $\dot{V}O_2 = 1.880 + 158.90\,\text{VeDBA}$, $n = 26$, Fig. 3b). In addition, we evaluated the feasibility of using these proxies (U, TBF, BBF, and DBA) to estimate the $\dot{V}O_2$ of Japanese sea bass. The AIC of the model using U as an explanatory variable was the lowest of all the models (Table 3). On the other hand, the model using BBF as an explanatory variable had the highest AIC value. A significant linear relationship between *TBF* and U was fitted with a regression line ($U = 0.884\,\text{TBF} - 0.667$, $R^2 = 0.932$, $F = 156.444$, $n = 26$, $P < 0.0001$, Fig. 4a). There was also a significant linear relationship between BBF calculated by lateral acceleration and U ($U = 0.706\,\text{BBF} - 0.330$, $R^2 = 0.848$, $F = 64.393$, $n = 26$, $P < 0.0001$, Fig. 4b). Furthermore, there was also a significant linear relationship between BBF and TBF (TBF $= 0.815\,\text{BBF} + 0.346$, $R^2 = 0.949$, $F = 215.170$, $n = 26$, $P < 0.0001$, Fig. 4c). On the other hand, there was an exponential relationship between VeDBA and U ($R^2 = 0.737$, $F = 32.231$, $n = 26$, $P < 0.001$, Fig. 5). The relationship was described by the following equation [16]:

$$\text{VeDBA} = 0.0057\exp(1.0035U). \tag{7}$$

The SMR when the swimming speed was zero was calculated as 2.26 mg O_2 kg^{-1} min^{-1} using Eq. 2 (Fig. 2a). The SMR in the models including TBF and BBF as explanatory variables was estimated using the activity value when the swimming speed was zero. SMR$_{TBF}$ and SMR$_{BBF}$ were found to be similar to SMR (2.29 and 2.39 mg O_2 kg^{-1} min^{-1}, respectively). The calculated values for COT$_{min}$ and U_{opt} were 2390 J kg^{-1} km^{-1} and 1.5 BL s^{-1}, respectively (Fig. 6). VO$_2$ at U_{opt} was then calculated as 6.11 mg O_2 kg^{-1} min^{-1} using Eq. 2. Therefore, the daily metabolic rate (DMR) when fish were not swimming (SMR) and when the fish swam at U_{opt} (AMR$_{opt}$) were estimated as 45.9 and 124.0 kJ kg^{-1} day^{-1}, respectively (Fig. 8b).

Calorific values of prey items and metabolic rate of Japanese sea bass

Calorific values of seven prey species (6 fishes and 1 prawn)—Japanese anchovy *Engraulis japonicus*, Japanese sardine *Sardinops melanostictus*, Japanese jack mackerel *Trachurus japonicus*, spotnape ponyfish *Nuchequula nuchalis*, sweetfish *Plecoglossus altivelis altivelis*, grey mullet *Mugil cephalus*, and freshwater prawn *Macrobrachium*

Fig. 2 Relationship between oxygen consumption rate ($\dot{V}O_2$) and **a** swimming speed (U), **b** tail beat frequency (TBF) observed in video recordings, or **c** body beat frequency (BBF) calculated from lateral acceleration. *Solid curves* indicate the relationship between $\dot{V}O_2$ and **a** U ($\dot{V}O_2 = \exp(0.815 + 0.686\ U)$, $n = 26$), **b** TBF ($\dot{V}O_2 = \exp(0.292 + 0.632\ \text{TBF})$, $n = 26$), or **c** BBF ($\dot{V}O_2 = \exp(0.467 + 0.518\ \text{BBF})$, $n = 26$), respectively. Each *symbol* on the plot indicates a fish
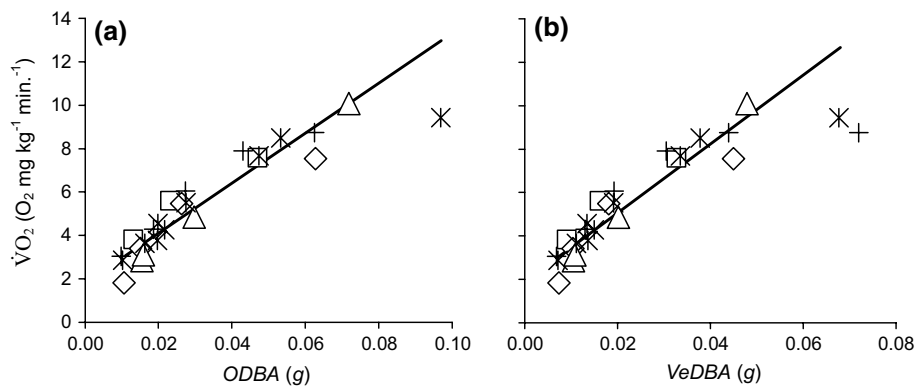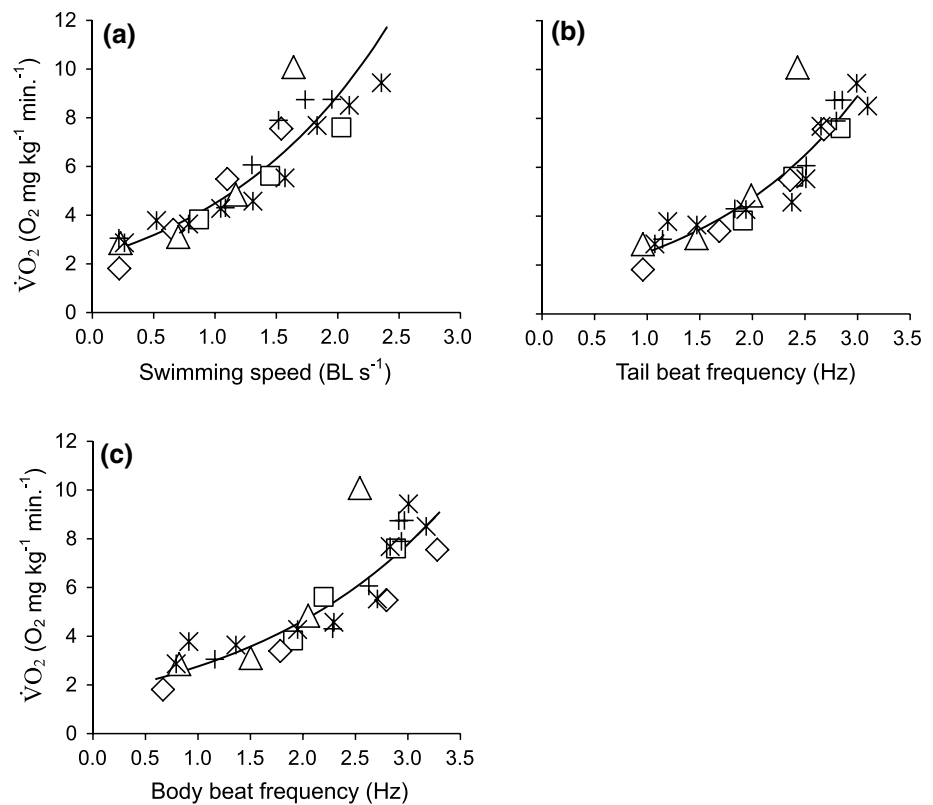
Fig. 3 Relationship between oxygen consumption rate ($\dot{V}O_2$) and **a** overall dynamic body acceleration (ODBA) or **b** vectorial dynamic body acceleration (VeDBA) calculated from the triaxial acceleration. *Solid lines* indicate the relationship between $\dot{V}O_2$ and **a** ODBA ($\dot{V}O_2 = 1.794 + 115.30\ \text{ODBA}$, $n = 26$) or **b** VeDBA ($\dot{V}O_2 = 1.880 + 158.90\ \text{VeDBA}$, $n = 26$), respectively. Each *symbol* on the plot indicates a fish

nipponense—were measured (Fig. 7a). The calorific values per g dry mass of the various species differed significantly (Kruskal–Wallis test, $P < 0.05$, $df = 6$). The calorific value per g dry mass of sweetfish *Plecoglossus altivelis altivelis* was highest amongst the prey species tested. However, the mean dry mass of the prey species ranged from 1.51 ± 0.79 g (grey mullet) to 10.68 ± 1.06 g (Japanese jack mackerel) (Fig. 7b). In terms of the whole calorific value of each prey species, Japanese sardine (229.4 ± 19.6 kJ) and

Japanese jack mackerel (218.9 ± 30.2 kJ) were higher than those of the other species (Fig. 8a).

Discussion

Japanese sea bass adopted three different swimming styles—unsteady, steady, and burst-and-glide swimming—by modulating U and TBF (Table 2). It was assumed that

Table 3 Generalized linear mixed models that use fish activity parameters (*U*, TBF, BBF, ODBA, and VeDBA) to describe $\dot{V}O_2$ (gamma error distribution)

Variable	*a*	*b*	Link	AIC	ΔAIC
U	0.815	0.686	log	71.52	–
TBF	0.292	0.632	log	72.32	0.80
BBF	0.497	0.518	log	77.90	6.38
ODBA	1.794	115.30	identity	75.19	3.67
VeDBA	1.880	158.90	identity	75.70	4.18

ΔAIC indicates the difference in AIC value between each model and the best model. In all models, the ID number of the fish was considered a random effect

these swimming styles are selected for various situations (e.g., resting, migration, chasing, and escaping). Although it is difficult to observe the behavior of fish under natural conditions, the animal-borne device used in this work can measure their movements and convert them into time-series data. Our results showed a linear relationship between TBF, BBF, and *U* (Fig. 4). Therefore, we can identify the swimming styles (unsteady, steady, and burst-and-glide swimming) using the relationships between swimming style and *U*, TBF, and BBF under natural conditions (Fig. 4; Table 2). In addition, the activity parameters of the fish—*U*, TBF, and BBF—were correlated with the oxygen

consumption rate (Fig. 2). We evaluated the feasibility of using these proxies (*U*, TBF, BBF, ODBA, and VeDBA) to estimate the $\dot{V}O_2$ of Japanese sea bass under natural conditions in future studies. Upon comparing the AIC values of the models, the model including *U* as the explanatory variable was found to have the lowest AIC, while the model including TBF as the explanatory variable had a similar AIC value to the *U* model (Table 3). This suggests that *U* and TBF are the best proxies to estimate $\dot{V}O_2$. On the other hand, the models that included ODBA and VeDBA as explanatory variables had higher AICs than the *U* and TBF models. The ODBA and VeDBA models had similar AIC values. This result is similar to those noted in previous studies [15, 16]. The model including BBF as the explanatory variable had a higher AIC than the DBA models. Dynamic body acceleration (DBA) parameters (e.g., VeDBA and ODBA) are widely accepted as proxies for animal activity and are used to estimate energy expenditure. However, the value of DBA is affected by both the frequency and the amplitude of animal movement. If the experimental conditions (such as the location of the accelerometer on the body of the fish and the size of the fish) vary, the calculated value of DBA could vary between individuals that are presenting the same activity level. For example, the results of the present study were compared with those obtained in a previous study [16]. In the present study, an accelerometer

Fig. 4 Relationship between **a** swimming speed (*U*) and tail beat frequency (TBF) observed in video recordings, **b** *U* and body beat frequency (BBF) calculated by lateral acceleration, or **c** TBF and BBF. *Solid lines* indicate the best-fitting regression [**a** $U = 0.884$ TBF $- 0.667$, $n = 26$, $R^2 = 0.932$; **b** $U = 0.706$ BBF $- 0.330$, $n = 26$, $R^2 = 0.848$; **c** TBF $= 0.815$ BBF $+ 0.346$, $n = 26$, $R^2 = 0.949$]. The *dotted line* in **a** indicates the regression line (TBF $= 0.56 + 1.33\ U$, $R^2 = 0.91$) for European sea bass *Dicentrarchus labrax*, as reported by Herskin and Steffensen [32]. Each *symbol* on the plot indicates a fish
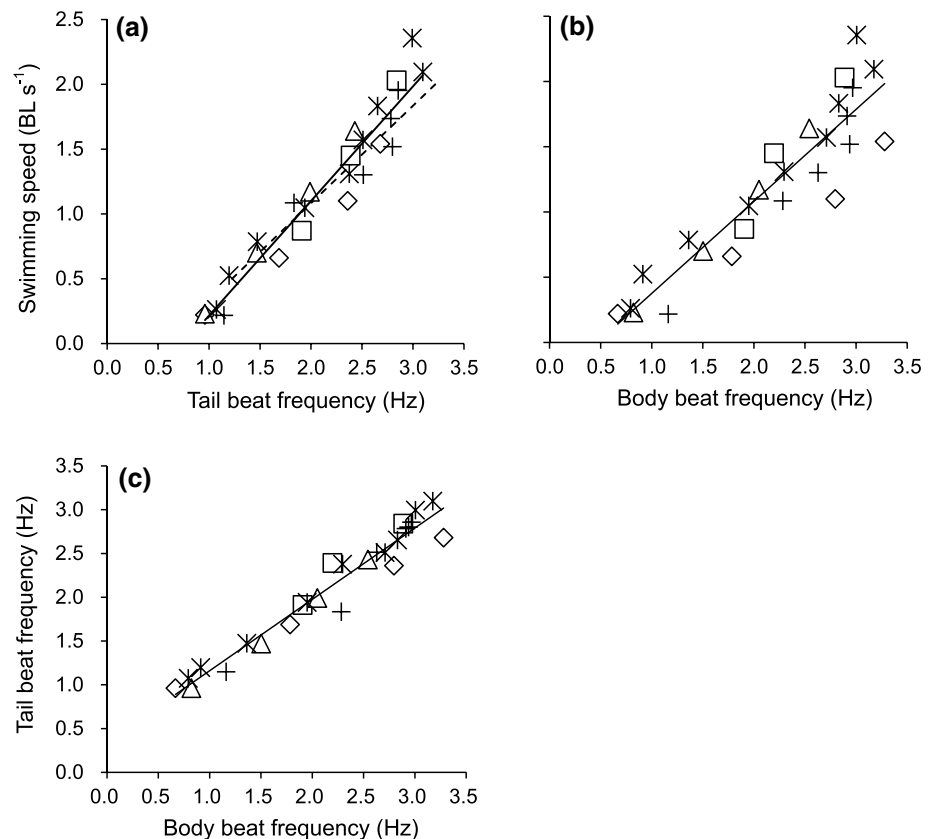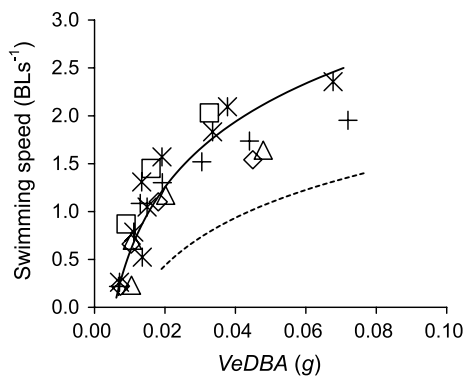
Fig. 5 Relationship between swimming speed (*U*) and vectorial dynamic body acceleration (VeDBA). The *solid curve* indicates the best-fitting regression [VeDBA = 0.0056 exp(1.0014 *U*), $n = 26$, $R^2 = 0.737$]. The *dotted curve* indicates the regression line (VeDBA = 0.0109 exp(1.3911 *U*), $R^2 = 0.870$) for European sea bass *Dicentrarchus labrax*, as reported by Wright et al. [16]. Each *symbol* on the plot indicates a fish
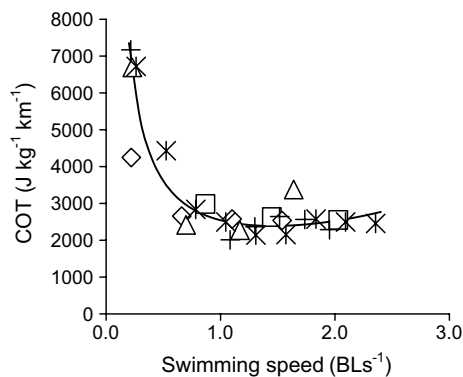

Fig. 6 The relationship between the cost of transport (COT; J kg^{-1} km^{-1}) and the swimming speed (*U*). The COT was minimized when the swimming speed was 1.5 BL s^{-1} (COT$_{min}$: 2390 J kg^{-1} km^{-1}). Each *symbol* on the plot indicates a fish

was deployed on the back of each Japanese sea bass tested (344–461 mm in total length, Table 1), whereas an accelerometer was inserted into the body cavity of the European sea bass *Dicentrarchus labrax* (523 ± 21 mm in total length) in a previous study. The VeDBA needed to attain a particular swimming speed differed greatly between the two experiments (Fig. 5). This point should be considered when comparing estimated energy expenditures by DBA obtained in different studies. On the other hand, swimming speed, TBF, and BBF may be less affected by experimental conditions. The relationship between TBF and *U* for European sea bass (288 ± 4 mm in total length) as reported by another previous study [32] was consistent with the relationship observed for Japanese sea bass in the present study (Fig. 4a). Therefore, we are able to estimate a robust

value for the energy expenditure using parameters such as *U*, TBF, and BBF. However, BBF did not completely correspond to TBF in our experiment (Fig. 4c). The value of BBF tended to be lower than the value of TBF at slow swimming speeds (Fig. 5b). This bias was likely caused by the difficulty involved in detecting oscillations of the body when the fish swam slowly, especially when the TBF was less than 1.2 Hz (Table 2). Therefore, we must be careful to take this into account when we estimate energy expenditure using BBF.

The $\dot{V}O_2$ when *U* is zero (SMR) was estimated to be 2.26 mg O$_2$ kg^{-1} min^{-1} using Eq. 2 (Fig. 2a). Similar values were obtained from other activity indices. SMR$_{TBF}$ and SMR$_{BBF}$ were estimated to be 2.29 and 2.39 mg O$_2$ kg^{-1} min^{-1}, respectively. The SMR was found to be 45.9 kJ kg^{-1} day^{-1} at a water temperature of 20 °C using the oxycalorific value (14.1 J mg O$_2^{-1}$ [4]). The estimated SMR of Japanese sea bass was close to corresponding values reported in previous studies. Yasuda et al. [33] reported that the SMR of red sea bream *Pagrus major* was 46.7 kJ kg^{-1} day^{-1} at 20 °C. Claireaux et al. [5] reported that the SMR of juvenile European sea bass *Dicentrarchus labrax* was 30.4 ± 7.2 and 38.7 ± 9.1 kJ kg^{-1} day^{-1} at 18 and 22 °C, respectively. Steinhausen et al. [10] reported that the SMR of saithe *Pollachius virens* and whiting *Merlangius merlangus* was 24.2 and 24.4 kJ kg^{-1} day^{-1} at 10 °C, respectively. SMR was found to be affected by water temperature [4, 5]. Q_{10} is an alternative index of temperature sensitivity transformed by the Arrhenius equation. Clarke and Johnston [34] reported that the temperature sensitivity, i.e., the Q_{10} value, of resting oxygen consumption in a range of teleost fishes (69 species) was 1.83. Therefore, the SMR in saithe and whiting was converted to 44.3 and 44.7 kJ kg^{-1} day^{-1} at 20 °C using the Q_{10} value. The SMR estimated in the present study is comparable with those results.

The optimum swimming speed (U_{opt}) of Japanese sea bass was estimated to be 1.5 BL s^{-1} (Fig. 6). This value was in the range of U_{opt} values reported for 9 teleost fish species that swim with lateral undulation of the body and caudal fin (0.7–2.8 BL s^{-1}) by Videler [4]. The COT$_{min}$ of Japanese sea bass (2390 J kg^{-1} km^{-1}) when it swam at U_{opt} was similar to those reported for other fishes with a similar body shape (subcarangiform) [35]. Videler [4] reported that the COT$_{min}$ of striped bass *Morone saxatilis* was 3136 J kg^{-1} km^{-1} at 15 °C when the swimming speed was 1.7 BL s^{-1}. Beamish [36] reported that the COT$_{min}$ of largemouth bass *Micropterus salmoides* was 2058 J kg^{-1} km^{-1} at 15 °C when the swimming speed was 1.9 BL s^{-1}. On the other hand, the COT$_{min}$ of European eel *Anguilla anguilla*, which has a different body shape (anguilliform), was 522–705 J kg^{-1} km^{-1} at 18–19 °C when the swimming speed was 0.74–1.02 BL s^{-1} [37].
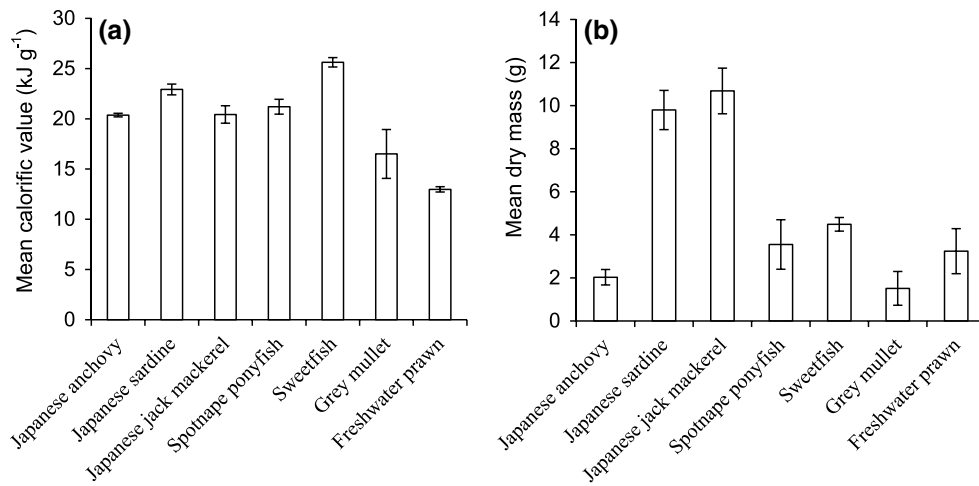
Fig. 7 **a** Mean calorific value per g dry mass and **b** the mean dry mass for each of the seven prey species examined. *Error bar* indicates one standard deviation
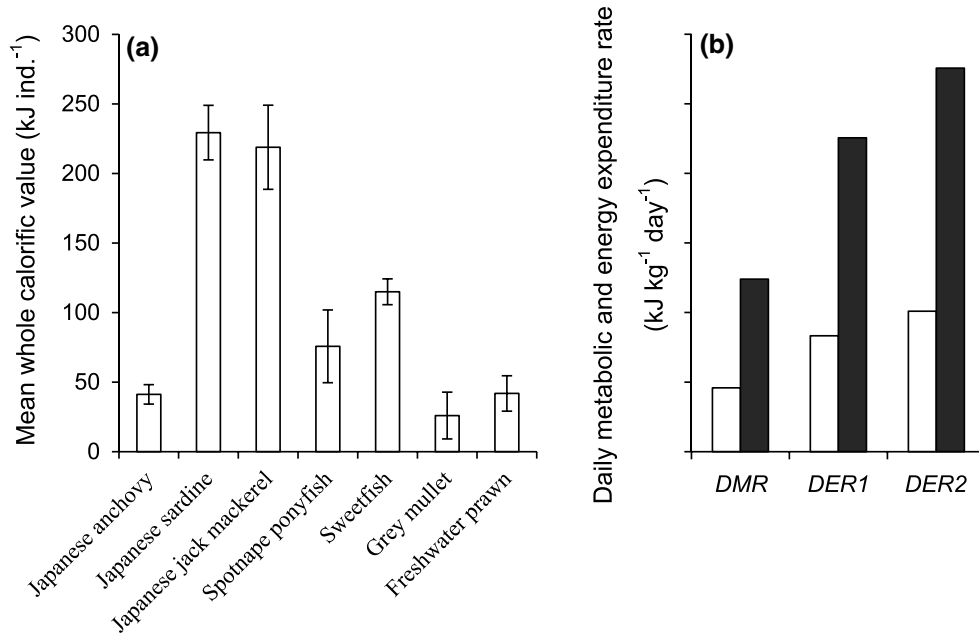

Fig. 8 **a** Mean whole calorific value of each prey species per individual, and **b** daily metabolic rate (DMR) and daily energy requirement (DER) of Japanese sea bass, as estimated from the respirometry measurements. *Error bar* indicates one standard deviation. The *col-*

umns indicate the DMR and the DER at the standard metabolic rate (SMR, *open*) and the active metabolic rate (AMR$_{opt}$, *closed*), respectively. *DER1* and *DER2* were calculated by combining the estimated components of the energy budget shown in Table 5

Adult European eels are well known to migrate long distances to the Sargasso Sea for spawning. The Japanese sea bass shows a similar swimming ability to other coastal fish, but its COT$_{min}$ was higher than that of the long-distance swimmer (*A. anguilla*). These results suggest that Japanese sea bass is adapted to the coastal area, and might not swim long distances.

Miyahara et al. [23] investigated the stomach contents of Japanese sea bass and reported its feeding habits in the

Harima-nada water area in Japan. As Japanese sea bass mature, they became more piscivorous. The main prey of adult Japanese sea bass include Japanese sardine *Sardinops melanostictus*, Japanese anchovy *Engraulis japonicus*, and Japanese jack mackerel *Trachurus japonicus* [23]. In this study, Japanese sardine and Japanese jack mackerel possessed higher calorific values than the daily metabolic rate (DMR) of Japanese sea bass per day (Fig. 8b). However, organisms cannot use all of the calories contained in their

Table 4 Details of prey items of Japanese sea bass

Prey item	Body length (mm)	Dry mass (g)	Whole calorific value (kJ)
Japanese anchovy (3) *Engraulis japonicus*	125 ± 8	2.03 ± 0.36	41.3 ± 7.0
Japanese sardine (5) *Sardinops melanostictus*	155 ± 6	9.80 ± 0.91	229.4 ± 19.6
Japanese jack mackerel (3) *Trachurus japonicus*	153 ± 7	10.68 ± 1.06	218.9 ± 30.2
Spotnape ponyfish (3) *Nuchequula nuchalis*	106 ± 6	3.55 ± 1.15	75.8 ± 26.2
Sweetfish (3) *Plecoglossus altivelis*	110 ± 2	4.49 ± 0.32	115.0 ± 9.3
Grey mullet (3) *Mugil cephalus*	93 ± 13	1.51 ± 0.79	26.0 ± 16.8
Freshwater prawn (3) *Macrobrachium nipponense*	93 ± 9	3.24 ± 1.05	41.9 ± 12.7

Mean ± S.D. Each number in parentheses in the "Prey item" column is the total number of samples of that prey species

prey. Assimilation efficiency must be considered when calculating energy expenditure. Hatanaka and Sekino [30] reported that daily feeding rates per body mass in wet tissue (when the daily growth rate was zero) corresponded to 2.45–2.97 % of Japanese sea bass body mass, so the energy gains from prey fish (Japanese anchovy) could be 83.3–100.9 kJ kg^{-1} day^{-1}. Previously, total metabolism R was subdivided into three components: R_S, the standard metabolic rate (SMR); R_A, the energy required for swimming and activity; and R_F, the energy required for the processes of digestion, movement, and excretion of food items (i.e., the apparent specific dynamic action, SDA) [4, 38, 39]. Therefore, the components of the energy budget when P growth is zero are described by the following equation:

$$C = R_S + R_A + R_F + E. \tag{8}$$

In addition, it was reported that the ratio of energy intake C to excretion E is 1.0:0.3, i.e., the assimilation efficiency is 0.7 [39, 40]. Furthermore, when sea bass were resting during the feeding examination reported by Hatanaka and Sekino [30], R_A was assumed to be nearly zero. Therefore, we can finally estimate the SDR (R_F) using the equation (Table 4)

$$C = (R_S + R_F) + 0.3C. \tag{9}$$

R_S(SMR) had already been estimated using respirometory trials in the present study. Hence, the apparent SDA of Japanese sea bass was estimated to range from 12.1–24.7 kJ kg^{-1} day^{-1} under SMR conditions (Table 5). The apparent SDA then was estimated as 15–25 % of the energy intake. According to Beamish [41], the specific dynamic action (SDA) of largemouth bass *Micropterus salmoides* did not change across a range of swimming speeds from 1.4 to 2.5 BL s^{-1} (until the maximum swimming speed was achieved). The overall mean apparent SDA ± SD was

Table 5 Components of the energy budget (kJ kg^{-1} day^{-1}) of Japanese sea bass assuming a growth rate of zero

Fish condition	R_S	R_A	R_F	E	C
DER1 at SMR	45.9 (55)	0 (0)	12.4 (15)	25.0 (30)	83.3 (–)
DER1 at AMR$_{opt}$	45.9 (20)	78.1 (35)	33.8 (15)	67.6 (30)	225.5 (–)
DER2 at SMR	45.9 (45)	0 (0)	24.7 (25)	30.3 (30)	100.9 (–)
DER2 at AMR$_{opt}$	45.9 (17)	78.1 (28)	68.9 (25)	82.7 (30)	275.6 (–)

R_S standard metabolic rate, R_A energy required for swimming and activity, R_F specific dynamic action, E excretory products (feces and urine), and C the total quantity of prey energy consumed by Japanese sea bass, respectively. The feeding rate in each daily energy requirement (DER) was assumed to be 2.45 % (DER1) and 2.97 % (DER2) per body mass in the wet tissue, respectively [30]. Numbers in parentheses indicate the percentage of each component of C

14.19 ± 4.19 % of the energy ingested. In addition, the SDA varies from 5 to 20 % in other fish species [38]. Therefore, we also applied the percentage of SDA, 15–25 % of the energy intake, when the fish was in the SMR condition, and estimated each component of the energy budget when the fish was in the AMR$_{opt}$ condition (at a swimming speed of 1.5 BL s^{-1}) using the following equation:

$$C = R_S + \alpha C + 0.3C, \tag{10}$$

where α was set to either 0.15 or 0.25 according to the SDA estimation above. The daily energy requirement (DER) of Japanese sea bass then ranged from 83.3 (SMR) to 275.6 (AMR$_{opt}$) kJ kg^{-1} day^{-1} (Fig. 8b; Table 5). These results suggest that the energy expenditure of Japanese sea bass is comparable with the calories contained in a few prey fish, e.g., the wet tissue mass was 12.4–41.2 g in Japanese

sardine *Sardinops melanostictus* and 14.6–48.1 g in Japanese jack mackerel *Trachurus japonicas* in the present study. These values correspond to 0.4–1.3 fish (mean TL 155 ± 6 and 153 ± 7 mm, respectively). According to a feeding experiment and an investigation of stomach contents, Hatanaka and Sekino [25] reported that the maximum feeding rate (percentage of wet body mass) of Japanese sea bass (>1 year old) ranged from 4.4 to 5.4 %. The energy intake values for these feeding rates were converted to 1.3–1.6 fish (Japanese sardine) and 1.2–1.4 fish (Japanese jack mackerel) per day, respectively. On the other hand, if Japanese sea bass predate low-calorific prey, e.g., grey mullet *Mugil cephalus* or freshwater prawn *Macrobrachium nipponense*, they need to feed on approximately 3.3–11.1 or 2.0–6.6 individuals per day, respectively, to consume the same amount of energy.

We estimated the metabolic rates and energy requirements of Japanese sea bass under two conditions: not swimming (SMR) and swimming at the optimum speed (AMR_{opt}) at a water temperature of 20 °C. AMR_{opt} was 2.8 times as much as SMR. Although AMR_{opt} varies between species, it is commonly assumed that metabolism in the active condition ranges from zero to four (almost three) times the metabolism in the SMR condition [42, 43]. Therefore, it is necessary to measure the activity to estimate the metabolic rate under natural conditions. If we measure the activity of free-ranging Japanese sea bass, BBF measurements obtained with an accelerometer could allow us to estimate the energy expenditure of each fish.

References

1. Baum JK, Worm B (2009) Cascading top-down effects of changing oceanic predator abundances. J Anim Ecol 78:699–714
2. Frank KT, Petrie B, Choi JS, Leggett WC (2005) Trophic cascades in a formerly cod-dominated ecosystem. Science 308:1621–1623
3. Estes JA, Tinker MT, Williams TM, Doak DF (1998) Killer whale predation on sea otters linking oceanic and nearshore ecosystems. Science 282:473–476
4. Videler JJ (1993) Fish swimming. Chapman and Hall, London
5. Claireaux G, Couturier C, Groison AL (2006) Effect of temperature on maximum swimming speed and cost of transport in juvenile European sea bass (*Dicentrarchus labrax*). J Exp Biol 209:3420–3428
6. Beamish FWH (1978) Swimming capacity. In: Hoar W, Randall D (eds) Fish physiology. VII: Locomotion. Academic, London, pp 101–187
7. Brett JR (1964) The respiratory metabolism and swimming performance of young sockeye salmon. J Fish Res Board Canada 21:1183–1226
8. Brett JR (1965) The relation of size to rate of oxygen consumption and sustained swimming speed of sockeye salmon (*Oncorhynchus nerka*). J Fish Res Board Canada 22:1491–1501
9. Van den Thillart G, van Ginneken V, Körner F, Heijimans R, Van der Linden R, Gluvers A (2004) Endurance swimming of European eel. J Fish Biol 65:312–318
10. Steinhausen MF, Steffensen JF, Andersen NG (2005) Tail beat frequency as a predictor of swimming speed and oxygen consumption of saithe (*Pollachius virens*) and whiting (*Merlangius merlangus*) during forced swimming. Mar Biol 148:197–204
11. Clark TD, Sandblom E, Hinch SG, Paterson DA, Frappell PB, Farrel AP (2010) Simultaneous biologging of heart rate and acceleration, and their relationships with energy expenditure in free-swimming sockeye salmon (*Oncorhynchus nerka*). J Comp Physiol B 180:673–684
12. Wilson RP, White CR, Quintana F, Halsey LG, Liebsch N, Martin GR, Butler PJ (2006) Moving towards acceleration for estimates of activity-specific metabolic rate in free-living animals: the case of the cormorant. J Anim Ecol 75:1081–1090
13. Halsey LG, Green JA, Wilson RP, Frappell PB (2009) Accelerometry to estimate energy expenditure during activity: best practice with data loggers. Physiol Biochem Zool 82:396–404
14. Gleiss AC, Dale JJ, Holland KN, Wilson RP (2010) Accelerating estimates of activity-specific metabolic rate in fishes: testing the applicability of acceleration data-loggers. J Exp Mar Bio Ecol 385:85–91
15. Qasem L, Cardew A, Wilson A, Griffiths I, Halsey LG, Shepard ELC, Gleiss AC, Wilson RP (2012) Tri-axial dynamic acceleration as a proxy for animal energy expenditure; should we be summing values or calculating the vector? PLoS One 7:e31187. doi:10.1371/journal.pone.0031187
16. Wright S, Metcalfe J, Hetherington S, Wilson R (2014) Estimating activity-specific energy expenditure in a teleost fish, using accelerometer loggers. Mar Ecol Prog Ser 496:19–32
17. Tanaka H, Takagi Y, Naito Y (2001) Swimming speeds and buoyancy compensation of migrating adult chum salmon *Oncorhynchus keta* revealed by speed/depth/acceleration data logger. J Exp Biol 204:3895–3904
18. Kawabe R, Kawano T, Nakano N, Yamashita N, Hiraishi T, Naito Y (2003) Simultaneous measurement of swimming speed and tail beat activity of free-swimming rainbow trout *Oncorhynchus mykiss* using an acceleration data-logger. Fish Sci 69:959–965
19. Lowe CG (2002) Bioenergetics of free-ranging juvenile scalloped hammerhead sharks (*Sphyrna lewini*) in Kāne'ohe Bay, Ō'ahu, HI. J Exp Mar Bio Ecol 278:141–156
20. Murchie KJ, Cooke SJ, Danylchuk AJ, Suski CD (2011) Estimates of field activity and metabolic rates of bonefish (*Albula vulpes*) in coastal marine habitats using acoustic tri-axial accelerometer transmitters and intermittent-flow respirometry. J Exp Mar Bio Ecol 396:147–155
21. Secor DH, Ohta T, Nakayama K, Tanaka M (1998) Use of otolith microanalysis to determine estuarine migrations of Japanese sea bass *Lateolabrax japonicus* distributed in Ariake Sea. Fish Sci 64:740–743
22. Tanaka M, Kinoshita I (2002) Temperate bass and biodiversity—new perspective for fisheries biology. Koseisha-koseikaku, Tokyo **(in Japanese)**

23. Miyahara K, Ohtani T, Shimamoto N (1995) Feeding habitats of Japanese sea bass *Leteolabrax japonicus* in Harima-nada. Hyogo Suishi Kenpo 32:1–8 **(in Japanese with English abstract)**

24. Fujita S, Kinoshita I, Takahashi I, Azuma K (1988) Seasonal occurrence and food habits of larvae and juveniles of two temperate basses in the Shimanto estuary, Japan. Jpn J Ichthyol 35:5–10

25. Hatanaka M, Sekino K (1962) Ecological studies on the Japanese sea bass, *Lateolabrax japonicus*. I. feeding habit. Nippon Suisan Gakkaishi 28:851–856 **(in Japanese with English abstract)**

26. Kato M, Ikegami N (2004) Recent trend of stock and distribution of fishing ground of small scale trawl for Japanese sea bass *Lateolabrax japonicus* (Cuvier) in Tokyo bay. Bull Chiba Pref Fish Res Cen 3:17–30 **(in Japanese)**

27. Watanabe T (1965) Ecological distribution of eggs of common sea bass, *Lateolabrax japonicus* (Cuvier) in Tokyo bay. Nippon Suisan Gakkaishi 31:585–590 **(in Japanese with English abstract)**

28. Fuji T, Kasai A, Suzuki KW, Ueno M, Yamashita Y (2011) Migration ecology of juvenile temperate seabass *Lateolabrax japonicus*: a carbon stable-isotope approach. J Fish Biol 78:2010–2025

29. Hatanaka M, Sekino K (1962) Ecological studies on the Japanese sea bass. *Lateolabrax japonicus*. II. Growth. Nippon Suisan Gakkaishi 28:857–861 **(in Japanese with English abstract)**

30. Hatanaka M, Sekino K (1962) Ecological studies on the Japanese sea bass, *Lateolabrax japonicus*. III. Efficiency of production. Nippon Suisan Gakkaishi 28:949–954 **(in Japanese with English abstract)**

31. Sakamoto KQ, Sato K, Ishizuka M, Watanuki Y, Takahashi A, Daunt F, Wanless S (2009) Can ethograms be automatically generated using body acceleration data from free-ranging birds? PLoS One 4:e5379. doi:10.1371/journal.pone.0005379

32. Herskin J, Steffensen JF (1998) Energy savings in sea bass swimming in a school: measurements of tail beat frequency and oxygen consumption at different swimming speeds. J Fish Biol 53:366–376

33. Yasuda T, Komeyama K, Kato K, Mitsunaga Y (2012) Use of acceleration loggers in aquaculture to determine net-cage use and field metabolic rates in red sea bream *Pagrus major*. Fish Sci 78:229–235

34. Clarke A, Johnston NM (1999) Scaling of metabolic rate with body mass and temperature in teleost fish. J Anim Ecol 68:893–905

35. Lindsey CC (1978) Form, function, and locomotory habits in fish. In: Hoar WS, Randall DJ (eds) Fish physiology. VII: Locomotion. Academic, London, pp 1–100

36. Beamish FWH (1970) Oxygen consumption of largemouth bass, *Micropterus salmoides*, in relation to swimming speed and temperature. Can J Zool 48:1221–1228

37. Palstra A, Van Ginneken V, Van den Thillart G (2008) Cost of transport and optimal swimming speed in farmed and wild European silver eels (*Anguilla anguilla*). Comp Biochem Physiol A Mol Integr Physiol 151:37–44

38. Elliott JM (1976) The energetics of feeding, metabolism and growth of brown trout (*Salmo trutta* L.) in relation to body weight, water temperature and ration size. J Animal Ecol 45:923–948

39. Tytler P, Calow P (1985) Fish energetics: new perspectives. Johns Hopkins University Press, Baltimore

40. Elliott JM, Davison W (1975) Energy equivalents of oxygen consumption in animal energetics. Oecologia 19:195–201

41. Beamish FWH (1974) Apparent specific dynamic action of largemouth bass, *Micropterus salmoides*. J Fish Res Board Canada 31:1763–1769

42. Boisclair D, Leggett WC (1989) The importance of activity in bioenergetics models applied to actively foraging fishes. Can J Fish Aquat Sci 46:1859–1867

43. Ney JJ (1993) Bioenergetics modeling today: growing pains on the cutting edge. Trans Am Fish Soc 122:736–748